Available online at www.sciencedirect.com

SCIENCE DIRECT®

Optical Materials 22 (2003) 263–268

OPTICAL Materials

www.elsevier.com/locate/optmat

Cs_2HgCl_4 crystal as a new material for acoustooptical applications

M.V. Kaidan [a], A.V. Zadorozhna [a], A.S. Andrushchak [a], A.V. Kityk [b,*]

[a] *Institute of Physical Optics, Dragomanov Str. 23, L'viv 79005, Ukraine*
[b] *Department of Electrical Engineering, Institute for Computer Science, Technical University of Czestochowa,*
Al. Armii Krajowej 17, Częstochowa PL-42200, Poland

Received 3 May 2002; received in revised form 30 May 2002; accepted 25 October 2002

Abstract

The paper reports the basic acoustical (anisotropy of phase velocity V_i and obliquity angle θ), optical (transparency spectra, refractive indices n_i and photoelastic constants p_{ij}) and acoustooptical (figure of merit $M_2 = p_{\mathrm{ef}}^2\tilde{n}^6/\rho V^3$) parameters of Cs_2HgCl_4 crystals that are necessary for a design of acoustooptical devices. Substantial photoelastic effect ($p_{ij} \sim 0.17$–0.41 for $i,j = 1$–3) and low ultrasonic velocities ($V_i \sim 870$–2500 m/s) in Cs_2HgCl_4 crystals determine relatively high figure of merit M_2 for the isotropic acoustooptical diffraction. We have found that for certain geometries of acoustooptical interactions $M_2 \sim (85$–$114) \times 10^{-15}$ s^3/kg. The new material may be considered, therefore, as a candidate for applications in acoustooptical devices.

PACS: 42.70.−a; 42.70.Nq; 42.79.Jq; 78.20.−e
Keywords: Acousto-optical materials; Acoustical properties; Optical properties; Figure of merit

1. Introduction

Caesium mercury tetrachlorate (Cs_2HgCl_4) is an optically biaxial crystal. According to the results of X-ray diffraction analysis [1] it possess by β-K_2SO_4-type structure at room temperature with an orthorhombic space group of symmetry Pnma and four formulae units per unit cell. The structure is stable up to $T_i \approx 220$ K. Below this temperature a sequence of structural transformations into the incommensurate, ferroelastic and ferroelectric phases is known to occur [2–4]. All components of the elastic constant (C_{ij}) and the elastic compliance (S_{ij}) tensors were determined in a wide temperature range including the regions of phase transitions [5–7]. The Mach–Zehdner interferometer technique has been used to study the photoelastic properties of Cs_2HgCl_4 crystals at room temperature [8]. Substantial photoelastic effect and low ultrasonic velocities determine relatively high figure of merit M_2 in this system for certain geometries of acoustooptical interaction. Cs_2HgCl_4 crystals can be considered, therefore, as a new promising material for acoustooptical applications. In the present paper we report the basic acoustical, optical and acoustooptical parameters of this crystals that are necessary for a design of acoustooptical devices.

---

[*] Corresponding author.
E-mail address: kityk@ap.univie.ac.at (A.V. Kityk).

0925-3467/03/$ - see front matter © 2002 Elsevier Science B.V. All rights reserved.
doi:10.1016/S0925-3467(02)00286-0

2. Single crystal growth and crystallographic orientation

Single crystals of Cs_2HgCl_4 were grown from the melt by vertical Bridgman method. A starting composition of $HgCl_2$ and CsCl in a molar proportion of 1:2 and a slow growth rate of 0.2 mm/h were employed for the growth. The originally grown crystals were of cylindrical form with the diameter of 2.5 cm and with a typical length of 10 cm. We used the following crystallographic orientation: $c > a > b$ $(c \approx \sqrt{3}b)$, where a is the pseudohexagonal axis [1]. The elastic and photoelastic constants referred in the paper are presented according to an orthonormal set of axes $X = 1$, $Y = 2$, $Z = 3$, which, in the case of the orthorhombic structure, possess a standard orientation in respect to the principal crystallographic axes: $a \equiv X$, $b \equiv Y$, $c \equiv Z$.

3. Anisotropy of ultrasonic phase velocity and obliquity angle

The ultrasonic measurements of Cs_2HgCl_4 crystals have been performed by pulse-echo overlap method (see [9]) at the frequency of 10 MHz. The longitudinal and transverse ultrasound waves were excited in samples by $LiNbO_3$ transducers. The samples have been prepared in a rectangular form with a typical size of $5 \times 5 \times 5$ mm^3. In order to obtain all the components of the elastic constants tensor C_{ij} or elastic compliancy tensor $S_{ij} = [C_{ij}]^{-1}$ the longitudinal and transverse ultrasonic phase velocities were measured along three principal crystallographic directions [1 0 0], [0 1 0] and [0 0 1] as well as along the diagonal directions [1 1 0], [1 0 1] and [0 1 1]. The elastic constants have been derived by solving the Chrystoffel equation (a comprehensive description of this procedure see is given e.g. [10]). Table 1 lists the measured ultrasound velocities $V(\mathbf{q}, \mathbf{e})$ (where $\mathbf{q}$ is the wavevector and $\mathbf{e}$ is the polarization) and calculated elastic constants C_{ij} and elastic compliances S_{ij}. Figs. 1 and 2 show the dependences of the phase velocity V and the acoustic obliquity angle θ (the angle between phase and group velocity) on the direction of sound propagation as calculated in the principal crystallographic planes using the data of the Table 1. Low magnitude of the ultrasound wave velocities is peculiar for Cs_2HgCl_4 crystals. It determines sufficient angles of acoustooptical diffraction on both longitudinal and transverse acoustical modes. An acoustic obliquity is another important characteristic for designers of acoustooptical devises. One can see that the maximal angles θ are observed in the XY-plane. Their magnitudes are close to the obliquity angles observed in isostructural compounds Cs_2CdBr_4 and Cs_2HgBr_4 [10]. The plots for the XZ- and YZ-plane seem to be rather peculiar. The acoustic obliquity for quasilongitudinal (QL-) mode (YZ-plane) increases slightly, reaching its maximal value of about 4° at the angle $\beta = 63°$ to the Y-axis, whereas for quasitransverse (QT-) and pure transverse T-modes it does not exceed even $\theta = 1°$ for any arbitrary direction in the XZ-plane. This fact is not unusual since there is only a weak anisotropy of the phase velocities for QT- and T-mode in this plane. An additional advantage of Cs_2HgCl_4 crystals is their orthorhombic

Table 1
The acoustical wave velocity and elastic constants of Cs_2HgCl_4 crystals

Acoustic wave			Elastic constants	
Propagation, polarization	Mode	Velocity, m/s	C_{ij}, 10^9 N/m^2	S_{ij}, 10^{-12} m^2/N
[1 0 0], [1 0 0]	Longitudinal	2510	$C_{11} = 25.5$	$S_{11} = 62.86$
[0 1 0], [0 1 0]	Longitudinal	1910	$C_{22} = 14.8$	$S_{22} = 104.6$
[0 0 1], [0 0 1]	Longitudinal	1960	$C_{33} = 15.6$	$S_{33} = 100.2$
[0 1 0], [0 0 1]	Transverse	870	$C_{44} = 3.05$	$S_{44} = 325.7$
[1 0 0], [0 0 1]	Transverse	1060	$C_{55} = 4.54$	$S_{55} = 220.3$
[1 0 0], [0 1 0]	Transverse	870	$C_{66} = 3.04$	$S_{66} = 327.9$
[1 1 0], [1 1 0]	Quasilongitudinal	2151	$C_{12} = 10.3$	$S_{12} = -28.56$
[1 0 1], [1 0 1]	Quasilongitudinal	2250	$C_{13} = 10.7$	$S_{13} = -28.85$
[0 1 1], [0 1 1]	Quasilongitudinal	1894	$C_{23} = 7.81$	$S_{23} = -32.66$

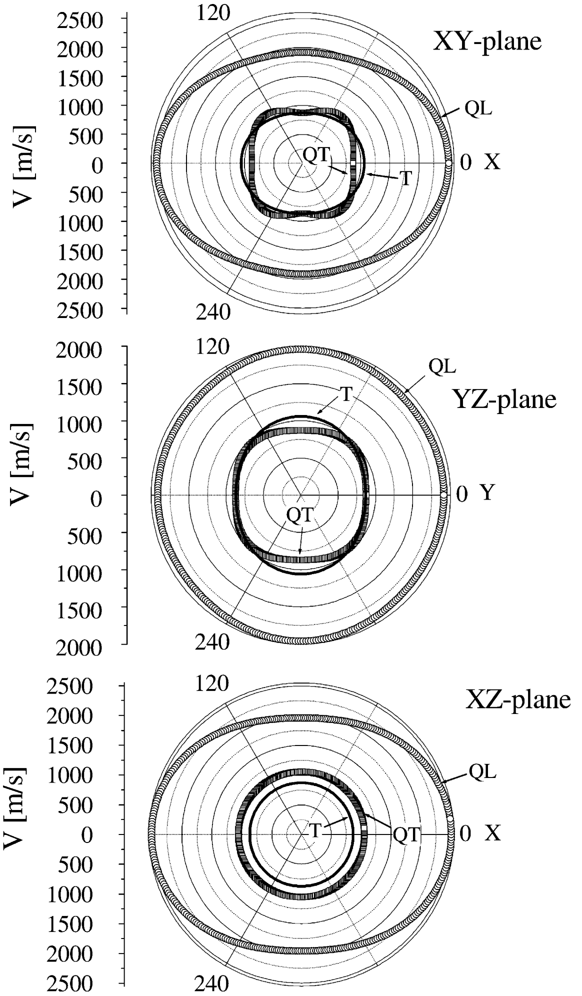

Fig. 1. The dependence of the phase velocity on the direction of sound propagation in the principal crystallographic *XY*-, *XZ*- and *YZ*-plane of Cs_2HgCl_4 crystals.

symmetry. Due to this reason no acoustic obliquity occurs when the acoustical waves propagate along the principal crystallographic directions (see Fig. 2, $\theta = 0$ at α, β or $\gamma = 90n$; $n = 0, 1, 2 \ldots$). Hence, the use of such sample geometries are preferable in design of acoustooptical devices.

4. Optical transparency and refractive indices

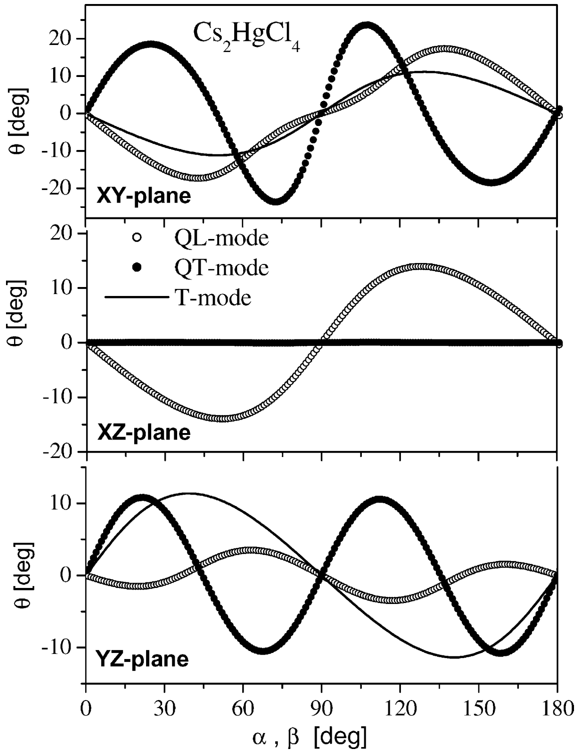

Fig. 2. The dependence of the acoustic walkoff angle θ on the direction of sound propagation in the principal crystallographic *XY*-, *XZ*- and *YZ*-plane of Cs_2HgCl_4 crystals.

Adsorption spectra have been obtained in two-stage geometry by using spectrophotometers SF-40 (200–900 nm), SPECORD M40 (880–2520 nm) and SPECORD 75IR (2500–25 000 nm). Fig. 3 shows the adsorption spectra of Cs_2HgCl_4 as measured in the spectral range 200–15 000 nm. The UV-absorption edge at about 310 nm is caused by inter-band transitions between the higher valence band formed prevailingly by 3p-Cl orbitals and bottom of the conduction band that is caused by the 6s-Hg terms. The ionic chemical bonds are dominated, so the covalence hybridization is relatively low and the corresponding absorption edge may be described within the approach developed for the typical ionic crystals like the NaCl. Concerning the two IR bands they cannot be cause by relatively heavy Hg and Cs atoms. Their origin is likely related to impurities or uncontrolled hydrogen-group atoms. The Cs_2HgCl_4 crystals are thus well transparent in the upper ultraviolet, visible and near infra-red regions of optical spectra that is substantial for most acoustooptical applications.

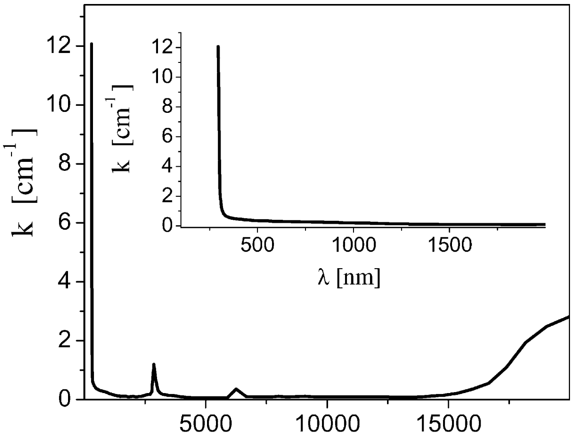

Fig. 3. The absorption spectra of Cs_2HgCl_4 crystals.

The refractive indices of Cs_2HgCl_4 were measured by Obreimov's immersion method, which gives the following values for the principal refractive indices ($\lambda = 632.8$ nm): $n_1 = 1.6498$, $n_2 = 1.6690$ and $n_3 = 1.6491$. The wavelength dependences of the principle refractive indices are shown in the Fig. 4. For all of them the system manifests the dispersion of the normal type.

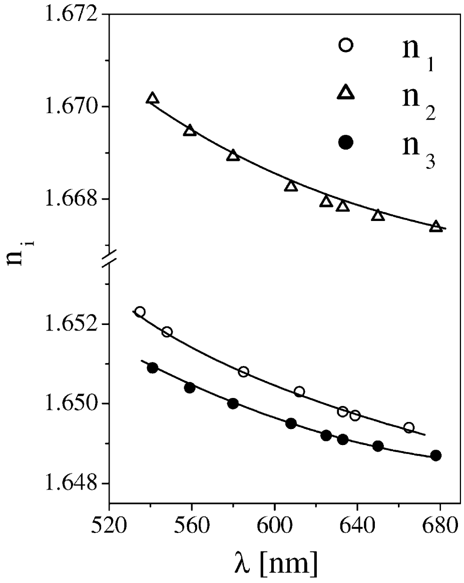

Fig. 4. The dispersion of the principal refractive indices of Cs_2HgCl_4 crystals.

5. Photoelastic constants and figure of merit M_2

The piezooptical measurements were performed at room temperature using a He–Ne laser ($\lambda = 632.8$ nm) and Mach–Zehdner interferometer technique [11,12]. Clearly, such a procedure has an advantage comparing to conventional acoustooptical methods since one determines both the magnitude and the sign of the piezooptical constants π_{im}. The induced changes of the optical path $\delta\Delta_{ikm}$ have been measured in order to obtain the piezooptical constants π_{im} [8]. They have been calculated using the following expressions:

$$\pi_{im} = -\frac{2\delta\Delta_{ikm}}{\sigma_m t_k n_i^3} + \frac{2S_{km}(n_i - 1)}{n_i^3}, \quad (i, m = 1, 2, 3); \tag{1}$$

$$\begin{aligned} \pi_{rr} &= -4n_r^{-3}\left(\frac{\delta\Delta_{r\bar{r}r}}{t_{\bar{r}}\sigma_r} - \frac{\delta\Delta_{\bar{r}r\bar{r}}}{t_r\sigma_{\bar{r}}}\right) \\ &\quad + n_r^{-3}(n_r - 1)(S_{ii} + S_{jj} + 2S_{ij} - S_{rr}) \\ &\quad - (\pi_{ii} + \pi_{ij} + \pi_{ji} + \pi_{jj})/2; \\ r &= 9 - i - j = 4, 5, 6; \quad i \neq j = 1, 2, 3, \\ n_r &= \sqrt{2}n_i n_j/\sqrt{n_i^2 + n_j^2}, \end{aligned} \tag{2}$$

where σ_m is the mechanical stress, n_i and n_j are the principal refractive indices, t_k and t_r are the sample thickness along the direction of light propagation; S_{km} is the elastic compliance, 4, 5 and 6 indicate the diagonal directions between the principal crystallographic axes (Y, Z), (X, Z) and (X, Y), respectively. As follows from Eq. (1), the piezooptical effect is presented here by two terms, which correspond to a direct (photoelastic) and non-direct (elastic) contributions, respectively. The sign of the induced values $\delta\Delta_{ikm}$ and, therefore, the sign of the piezooptical constants π_{im} were determined using the criteria described in [11]. The measurements of the piezooptical constants $\pi_{im} = \pi_{qlrs}$ ($i \equiv ql$, $m \equiv rs$; $i, m = 1, 2, 3$; $1 \equiv 11$, $2 \equiv 22$, $3 \equiv 33$) and $\pi_{im} = 2\pi_{qlrs}$ ($i \equiv ql$, $m \equiv rs$; $i = m = 4, 5, 6$; $4 \equiv 23 \equiv 32$, $5 \equiv 13 \equiv 31$, $6 \equiv 12 \equiv 21$) were performed either on rectangular samples oriented along the principal crystallographic directions (direct-cut samples; for $i, m = 1, 2, 3$) or on the X/45°-, Y/45°- and Z/45°-cut prepared again in a rectangular form (for $i = m = 4$, 5, 6). The samples were typically $\sim 5 \times 5 \times 5$ mm^3 in size. Piezooptical measurements were performed on electrically unshorted samples, i.e. at the constant electric displacement. The photoelastic constants p_{in} of Cs_2HgCl_4 crystals have been calculated using the relation $p_{in} = \pi_{im}C_{mn}$, where C_{mn} are the elastic constants taken from [7]. They are presented in Table 2. It is amazing that the photoelastic effect in these crystals is stronger comparing to well known acoustooptical materials such as TeO_2 or $PbMoO_4$, for which the largest photoelastic constants are $p_{13} = 0,34$ and $p_{33} = 0,30$ [13], respectively.

The figure of merit M_2 is one of the most important parameters that characterises the acoustooptical interaction [13] (a comprehensive description is given also in books [14,15]). Table 1 lists the magnitudes of M_2 for Cs_2HgCl_4 crystals, which have been calculated for the principal crystallographic directions according to the formulae:

$$M_2 = p_{\mathrm{ef}}^2 \tilde{n}^6 / \rho V^3, \tag{3}$$

where we consider $\tilde{n}^6 \approx (n_{\mathrm{i}} n_{\mathrm{d}})^3$ ($\tilde{n}$ is the average refractivity, n_{i} and n_{d} are the refraction indices of the incident and diffracted light, respectively), ρ is the crystal density, V is the ultrasonic wave velocity, p_{ef} is the effective photoelastic constant. For the comparison, the data for well-known acoustooptical material α-HJO_3 [16,17] are presented in Table 2 as well. It is amazing that both these crystals have the same orthorhombic symmetry and are water-soluble. Strong photoelastic effect and low ultrasonic velocities in Cs_2HgCl_4 (for comparison the longitudinal acoustic L-modes in α-HJO_3 crystals have the following velocities: $V_{11} = 3560$ m/s and $V_{22} = 2890$ m/s [15]) cause substantial figure of merit (i.e. high diffraction efficiency) comparing to α-HJO_3 crystals in the case of the isotropic diffraction. The priority for Cs_2HgCl_4 crystals is the acoustooptical interaction between the acoustic L-modes V_{22} or V_{33} and optical wave polarized along [1 0 0] (see Table 2). Those interactions are characterized by the figure of merit $M_2 = 114 \times 10^{-15}$ s^3/kg and $M_2 = 100 \times 10^{-15}$ s^3/kg, respectively. For comparison, the largest diffraction efficiency in α-HJO_3 ($M_2 = 83 \times 10^{-15}$ s^3/kg) appears in the isotropic acoustooptical interaction between the acoustic L-mode V_{33} and the optical wave polarized along [1 0 0].

The figure of merit M_2 is not so substantial for the anisotropic diffraction as one can see for several geometries of the acoustooptical interaction presented in Table 2. However, we do not exclude a possibility of larger diffraction efficiency in

Table 2
The calculated photoelastic constants p_{ef} and the figure of merit M_2 for Cs_2HgCl_4 crystals

Type of AO-diffraction	Polarization of optical wave		Acoustic wave			Effective coefficient, $p_{\mathrm{ef}} = p_{in}$	$M_2 \times 10^{15}$, s^3/kg	$M_2 \times 10^{15}$ for α-HIO_3, s^3/kg
	Incident light	Diffracted light	Propagation, polarization	Mode[a]	Velocity $V \times 10^{-3}$, m/s			
Isotropic	[1 0 0]	[1 0 0]	[1 0 0],[1 0 0]	L	2.51	$p_{11} = 0.40$	50	48
Isotropic	[1 0 0]	[1 0 0]	[0 1 0],[0 1 0]	L	1.91	$p_{12} = 0.40$	114	42
Isotropic	[1 0 0]	[1 0 0]	[0 0 1],[0 0 1]	L	1.96	$p_{13} = 0.39$	100	83
Isotropic	[0 1 0]	[0 1 0]	[1 0 0],[1 0 0]	L	2.51	$p_{21} = 0.26$	23	21
Isotropic	[0 1 0]	[0 1 0]	[0 1 0],[0 1 0]	L	1.91	$p_{22} = 0.29$	65	58
Isotropic	[0 1 0]	[0 1 0]	[0 0 1],[0 0 1]	L	1.96	$p_{23} = 0.34$	85	78
Isotropic	[0 0 1]	[0 0 1]	[1 0 0],[1 0 0]	L	2.51	$p_{31} = 0.17$	9.0	46
Isotropic	[0 0 1]	[0 0 1]	[0 1 0],[0 1 0]	L	1.91	$p_{32} = 0.19$	26	33
Isotropic	[0 0 1]	[0 0 1]	[0 0 1],[0 0 1]	L	1.96	$p_{33} = 0.25$	41	63
Anisotropic	[0 1 0]	[0 0 1]	[0 1 0],[0 0 1]	T	0.87	$p_{44} = -0.034$	7.1	18
Anisotropic	[1 0 0]	[0 0 1]	[1 0 0],[0 0 1]	T	1.06	$p_{55} = -0.026$	3.8	25
Anisotropic	[1 0 0]	[0 1 0]	[1 0 0],[0 1 0]	T	0.87	$p_{66} = -0.032$	7.0	28

The figure of merit is calculated only for the principal crystallographic directions.

[a] L and T are the longitudinal and transverse acoustic waves, respectively.

Cs_2HgCl_4 crystals for the cases when the optical and acoustic waves propagate along non-principal crystallographic directions. A more detailed analysis would be quite useful in this case.

The advantage of Cs_2HgCl_4 crystals among the acoustooptical materials is the anisotropy of the acoustical and optical properties. This allows choosing an optimal their combination for design of acoustooptical devices. In particular, Cs_2HgCl_4 are optically biaxial crystals. Hence, they can be considered as promising materials in the design of acoustooptical cells with low optical losses, which may be achieved using sample geometries with a wide range of acoustooptical interaction angles [13]. The list of the materials of similar type with good acoustooptical properties is known to be rather short.

6. Conclusion

The paper reports the basic acoustical (anisotropy of phase velocity and obliquity angle), optical (transparency spectra, refractive indices and photoelastic constants) and acoustooptical (figure of merit M_2) parameters of Cs_2HgCl_4 crystals. Substantial photoelastic effect and low ultrasonic velocities in Cs_2HgCl_4 crystals determine relatively high figure of merit M_2 for the isotropic acoustooptical diffraction. We have found that for certain geometries of acoustooptical interactions $M_2 \sim 100\text{–}110 \times 10^{-15}$ s^3/kg. The new material may be considered, therefore, as a candidate for applications in acoustooptical devices.

References

[1] B.Sh. Bagautdinov, I.D. Brown, Yu.I. Yuzyuk, V.P. Dmitriev, Phys. Solid State 43 (2001) 350.

[2] V.P. Dmitriev, Yu.I. Yusyuk, A.V. Tregubchenko, E.S. Larin, V.V. Kirilenko, V.I. Pakhomov, Sov. Phys. Solid State 30 (1988) 704.

[3] S.N. Kallayev, V.V. Gladkii, V.A. Kirikov, I.K. Kamilov, Ferroelectrics 106 (1990) 299.

[4] V.V. Petrov, A.Yu. Halahan, V.G. Pitsyuga, V.E. Yachmenov, Sov. Phys. Solid State 30 (1988) 906.

[5] A.V. Kityk, O.M. Mokry, V.P. Soprunyuk, O.G. Vlokh, J. Phys.: Condens. Matter 5 (1993) 5189.

[6] A.V. Kityk, Ya.I. Shchur, A.V. Zadorozhna, I.B. Trach, I.S. Girnyk, I.Yu. Martynyuk-Lototska, O.G. Vlokh, Phys. Rev. B 58 (1998) 2505.

[7] A.V. Kityk, A.V. Zadorozhna, Ya.I. Shchur, I.Yu. Martynyuk-Lototska, O.G. Vlokh, Phys. Stat. Sol. (b) 210 (1998) 35.

[8] M.V. Kaidan, A.V. Zadorozhna, A.S. Andruschak, A.V. Kityk, Appl. Optics 41 (2002) 5341.

[9] E.P. Papadakis, in: W.P. Mason, R.N. Thurston (Eds.), Physical Acoustics, vol. 12, Academic, New York, 1976, p. 279.

[10] A.V. Kityk, A.V. Zadorozhna, Ya.I. Shchur, I.Yu. Martynyuk-Lototska, Ya. Burak, O.G. Vlokh, Australian J. Phys. 51 (1998) 643.

[11] B.G. Mytsyk, Ya.V. Pryriz, A.S. Andrushchak, Cryst. Res. Technol. 26 (1991) 931.

[12] N.A. Romanyuk, B.G. Mytsyk, L.N. Kulyk, Ukrainskii Fizicheskii Zhurnal 31 (1986) 354.

[13] B.I. Balakshyj, V.N. Parygin, L.E. Chirkov, Fizicheskie osnovy akusto-optiki, Izd. Radio i svjaz, Moscow, 1985.

[14] A. Korpel, Acousto Optics, second ed., Marcel Dekker, 1996.

[15] J. Xu, R. Stroud, Acousto-Optic devices: Principle, design and applications, John Willey & Sons, 1992.

[16] I.M. Silvestrova, N.S. Spiridonova, N.A. Moisejeva, Y.V. Pisarevskij, Acoustooptical properties of α-HJO_3 crystals, Preprint no. 365, Institut for Crystallography AN USSR, Moscow, 1991.

[17] D.A. Pinnow, R.W. Dixon, Appl. Phys. Lett. 13 (1968) 156.